Nonadiabatic features of electron pumping through a quantum dot in the Kondo regime

Liliana Arrachea
Departamento de Física de la Materia Condensada and BIFI, Universidad de Zaragoza, Pedro Cerbuna 12, 50009 Zaragoza, Spain

Alfredo Levy Yeyati and Alvaro Martin-Rodero
Departamento de Física Teorica de la Materia Condensada, Universidad Autónoma de Madrid, E-28048, Madrid, Spain

(Received 21 November 2007; revised manuscript received 3 February 2008; published 18 April 2008)

We investigate the behavior of the dc electronic current J^{dc} in an interacting quantum dot driven by two ac local potentials oscillating with a frequency Ω_0 and a phase lag φ. We provide analytical functions to describe the fingerprints of the Coulomb interaction in an experimental J^{dc} vs φ characteristic curve. We show that the Kondo resonance, at low temperatures, reduces the frequency range for the linear behavior of J^{dc} in Ω_0 to take place and determines the evolution of the dc current as the temperature increases.

DOI: 10.1103/PhysRevB.77.165326 PACS number(s): 72.10.Bg, 72.10.Fk, 73.63.−b

I. INTRODUCTION

We are presently witnessing an increasing interest in dc transport induced by pure ac fields. Quantum pumps, where transport is generated by applying harmonically time-dependent gates oscillating with a phase lag φ at the walls of semiconducting quantum dots, are paradigmatic examples realized in the laboratory.[1–3] On the other hand, the possibility of exploring the Kondo regime in semiconducting and carbon nanotube quantum dots provides a unique test system to understand the role of electronic correlations in quantum transport.[4,5] The combination of ac pumping mechanisms with many-body interactions constitutes a challenging avenue of research. On the experimental side these studies are likely to be feasible in the near future, since although these setups employ very slowly oscillating fields, great efforts are currently being devoted to increase the range of operational frequencies.[3] The use of superconducting junctions as ac generators seems to be a promising methodology in this direction.[6]

Since the celebrated proposals of Refs. 7 and 8 the "adiabatic approximations" have been at the heart of theoretical work on pumping in quantum dots driven at their walls.[9–11] Within these approximations the induced dc current J^{dc} is proportional to the pumping frequency Ω_0, describing the regime where $\Omega_0 \ll \tau^{-1}$, τ being the characteristic time for the electrons to travel through the dot. Few theoretical studies have addressed the problem of many-body interactions in quantum pumps.[12–15] Most of the work has been centered in adiabatic approximations,[12–14] and the electronic interactions are usually included within the slave boson mean-field approximation,[13] which does not properly account for inelastic many-body effects.

In the present work, we also focus on near-equilibrium regimes, where Ω_0 is lower than the Kondo temperature T_K, but we explore the effect of the interactions beyond the adiabatic regime. To this end we combine two methods: (i) the treatment of the interactions by a second-order self-energy as considered in Ref. 16, which has been a successful tool to study dc transport in the Kondo regime,[16,18] and (ii) the Keldysh Green's functions formalism with the Fourier representation of Ref. 17, which has been used to study models of noninteracting quantum pumps at arbitrary frequency.[17,19] We provide analytical expressions to identify the fingerprints of the interactions in the J^{dc} vs φ characteristic curve, which is the feature usually explored experimentally.[1] We anticipate that the development of Kondo resonance imposes limits on the range of frequencies for the $J^{dc} \propto \Omega_0$ behavior to be observed, while inelastic scattering induced by the interactions tends to restore this behavior.

The work is organized as follows. In the next section we present the model and technical details of the theoretical approach. We present results in Sec. IV. Section V is devoted to a summary and conclusions.

II. THEORETICAL FORMULATION

A. Model

We describe the quantum pump in terms of a generalized Anderson impurity model (see sketch of Fig. 1):

$$H(t) = \sum_{\alpha=L,R,k_\alpha,\sigma} \varepsilon_{k_\alpha} n_{k_\alpha,\sigma} - w_c \sum_{\alpha,k_\alpha,\sigma} (c^\dagger_{k_\alpha,\sigma} c_{l_\alpha,\sigma} + \text{H.c.}) - w \sum_{l=-1,\sigma}^{0} (c^\dagger_{l,\sigma} c_{l+1,\sigma} + \text{H.c.}) + \sum_{l=-1,\sigma}^{1} \varepsilon_l(t) c^\dagger_{l,\sigma} c_{l,\sigma} + U n_{0,\uparrow} n_{0,\downarrow}, \quad (1)$$

where $\varepsilon_l(t) = \delta_{l,-1}[E + V\cos(\Omega_0 t + \varphi)] + \delta_{l,1}[E + V\cos(\Omega_0 t)]$. A dot with Coulomb interaction U is inserted between two barriers of height E at which two ac fields are applied with amplitude V. The degrees of freedom of the reservoirs are denoted by k_α, where $\alpha = L, R$; the reservoirs are at equal chemical potential μ and temperature $T = 1/\beta$. The reservoirs

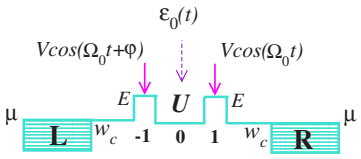

FIG. 1. (Color online) Sketch of the setup. The two external ac potentials and the induced potential at the interacting site are indicated with solid and dashed arrows, respectively.

are attached at the positions $l_\alpha = \pm 1$ of the central structure through hopping terms with amplitude w_c.

B. Charge currents

Following the procedure of Ref. 17 the dc current along the structure can be expressed as a sum of an *elastic* and an *inelastic* component as follows:

$$J^{\mathrm{dc}} = J^{\mathrm{el}} + J^{\mathrm{in}} = \sum_{k=-\infty}^{+\infty} \int_{-\infty}^{\infty} \frac{d\omega}{2\pi} [I^{\mathrm{el}}(k,\omega) + I^{\mathrm{in}}(k,\omega)], \quad (2)$$

where, adopting units with $e=\hbar=1$, and, to simplify, omitting explicit reference to the spin index,

$$I^{\mathrm{el}}(k,\omega) = 2[f(\omega - k\Omega_0) - f(\omega)]\Gamma(\omega)\Gamma(\omega - k\Omega_0) \sum_{l_\alpha, l'_\alpha = \pm 1} l_\alpha |\mathcal{G}_{l_\alpha, l'_\alpha}(k, \omega - k\Omega_0)|^2. \quad (3)$$

Here $\Gamma(\omega) = 2\pi |w_c|^2 \Sigma_{k_\alpha} \delta(\omega - \varepsilon_{k_\alpha})$ is the tunneling rate from the structure to the reservoirs, and $G_{l,l'}(k,\omega)$ is the kth Fourier coefficient of the retarded Green's function:

$$G^R_{l,l'}(t,t') = \sum_{k=-\infty}^{+\infty} e^{-ik\Omega_0 t} \int_{-\infty}^{+\infty} \frac{d\omega}{2\pi} e^{-i\omega(t-t')} \mathcal{G}_{l,l'}(k,\omega).$$

The elastic component takes into account processes where electrons propagate coherently along the dot structure, experiencing virtual absorption or emission of quanta of frequency Ω_0 at the pumping centers. The ensuing expression coincides with the noninteracting one, except for the fact that the retarded Green's function corresponds in the present case to the interacting system described by the full Hamiltonian (1). In contrast, the inelastic contribution accounts for processes in which electrons experience decoherence originating in the many-body interactions. It reads

$$I^{\mathrm{in}}(k,\omega) = 2 \sum_{k'=-\infty}^{+\infty} \mathrm{Re}\Big\{ \Gamma(\omega) \big[\lambda^{>}(\omega) \Sigma_0^{<}(k', \omega - k\Omega_0) - \lambda^{<}(\omega) \Sigma_0^{>}(k', \omega - k\Omega_0) \big] \Big(\sum_{l_\alpha = \pm 1} l_\alpha \times \mathcal{G}_{l_\alpha, 0}[k - k', \omega - (k-k')\Omega_0] \mathcal{G}^*_{l_{\alpha'}, 0}(k, \omega - k\Omega_0) \Big) \Big\}, \quad (4)$$

where $\lambda^{<}(\omega) = if(\omega)$ and $\lambda^{>}(\omega) = -i[1 - f(\omega)]$, which depend on the Fermi function $f(\omega) = 1/(e^{\beta(\omega-\mu)}+1)$. We have also introduced the Fourier representation of Ref. 17 in the lesser and greater self-energies $\Sigma_0^{<,>}(k,\omega)$, which describe the many-body effects due to the Coulomb interaction:

$$\Sigma_0^{<,>}(t,t') = \sum_{k=-\infty}^{+\infty} e^{-ik\Omega_0 t} \int_{-\infty}^{+\infty} \frac{d\omega}{2\pi} e^{-i\omega(t-t')} \Sigma_0^{<,>}(k,\omega).$$

III. TREATMENT OF THE COULOMB INTERACTION

A. Time-dependent Hartree-Fock approximation

While the above expressions are in principle exact, the many-body self-energies must be calculated at some level of approximation. The lowest order in the interaction U corresponds to the time-dependent Hartree-Fock (TDHF) approximation. The many-body problem is reduced to considering Hamiltonian (1) with $U=0$ and a renormalized level given by

$$\varepsilon_l^{\mathrm{TDHF}}(t) = \varepsilon_l(t) + \delta_{l,0} U \sum_{k=-\infty}^{+\infty} n_{0,\sigma}^{\mathrm{TDHF}}(k) e^{-ik\Omega_0 t}. \quad (5)$$

The Fourier components of the local particle density $n_{0,\sigma}^{\mathrm{TDHF}}(k)$ must be evaluated self-consistently. This level of perturbation theory leads to a vanishing inelastic contribution $I^{\mathrm{in}}(k,\omega)$ and it is not suitable for the description of Kondo physics. It is, however, interesting to notice that this simple approximation already introduces a nontrivial ingredient in the pumping problem; namely, the effective emergence of an additional pumping center in the interacting site (see Fig. 1).

B. Second-order self-energy approximation

In order to go beyond the TDHF description we consider the second-order self-energy (SOSE) given by the bubble diagram of Ref. 16 and generalize the procedure of that work to situations with a harmonic dependence on time. Concretely, we consider the following lesser and greater components of the self-energy:

$$\Sigma_0^{>,<}(k, t-t') = \pm iU^2 \sum_{k_1,k_2=-\infty}^{+\infty} G_0^{0,>,<}(k_1, t-t') \times [G_0^{0,>,<}(k_2, t-t')]^* G_0^{0,>,<}(k - k_1 + k_2, t - t'), \quad (6)$$

where the propagators are $G_0^{0,>,<}(k,\omega) \equiv G_{0,0}^{0,>,<}(k,\omega)$ with

$$G_{l,l'}^{0,>,<}(k,\omega) = \sum_{\alpha,k'} \mathcal{G}^0_{l,l_\alpha}(k+k', \omega - k'\Omega_0) \Lambda^{>,<}(\omega - k'\Omega_0) \times [\mathcal{G}^0_{l',l_\alpha}(k', \omega - k'\Omega_0)]^*,$$

$$G_{l,l'}^{0,>,<}(k, t-t') = \int_{-\infty}^{+\infty} \frac{d\omega}{2\pi} e^{-i\omega(t-t')} G_{l,l'}^{0,>,<}(k,\omega), \quad (7)$$

where $\mathcal{G}^0_{l,l'}(k,\omega)$ are the *nonequilibrium* retarded Green's functions, $\Lambda^{>,<}(\omega) \equiv \lambda^{>,<}(\omega)\Gamma(\omega)$ while $\mathcal{G}^0_{l,l'}(\omega)$ is the solution of the Dyson's equation corresponding to the Hamiltonian (1) with $U=0$, and

$$\varepsilon_l^{\mathrm{SOSE}}(t) = \varepsilon_l(t) + \delta_{l,0} \sum_{k=-\infty}^{+\infty} \varepsilon_0^{\mathrm{eff}}(k) e^{-ik\Omega_0 t}. \quad (8)$$

The Fourier components of the effective potential $\varepsilon_0^{\mathrm{eff}}(k)$, are determined self-consistently from the condition that the occupation of the interacting site evaluated within the SOSE approximation equals the one evaluated with (10), i.e.,

$$n_{0\sigma}^{\mathrm{SOSE}}(k) \equiv -i \int_{-\infty}^{+\infty} \frac{d\omega}{2\pi} G_0^{<}(k,\omega) = -i \int_{-\infty}^{+\infty} \frac{d\omega}{2\pi} G_0^{0,<}(k,\omega), \quad (9)$$

where the lesser Green's function of the first equality contains the full dressing by the self-energy:

$$G^{>,<}_{l,l'}(k,\omega) = \sum_{\alpha,k'} \mathcal{G}_{l,l_\alpha}(k+k',\omega-k'\Omega_0)\Lambda^{>,<}(\omega-k'\Omega_0) \times[\mathcal{G}_{l',l_\alpha}(k',\omega-k'\Omega_0)]^* + \sum_{k',k''} \mathcal{G}_{l,0}[k+k'-k'',\omega-(k'-k'')\Omega_0]\Sigma^{>,<}(k'',\omega-k'\Omega_0) \times[\mathcal{G}_{l',0}(k',\omega-k'\Omega_0)]^*, \quad (10)$$

while that of the second one corresponds to (7). The above procedure ensures the satisfaction of the Friedel-Langreth sum rule in the equilibrium limit.[16] Unfortunately, however, this procedure is not enough to ensure the conservation of the inelastic component of the current. The error in the estimate of the dc current due to the eventual violation of such conservation is, thus, bounded by the inelastic contribution of the self-energy ($\propto\Omega_0^2$).

The retarded self-energy is then obtained from

$$\Sigma_0^R(k,t-t') = \Theta(t-t')\left[\Sigma_0^<(k,t-t') - \Sigma_0^>(k,t-t')\right], \quad (11)$$

and it is introduced in the Dyson's equation: for the full dressed retarded Green's functions $\mathcal{G}_{l,l'}(k,\omega)$. The latter are evaluated by using the renormalization procedure of Ref. 17. The algorithm is combined with the use of fast Fourier transform between the variables $t-t' \leftrightarrow \omega$.

C. Low-amplitude and low-frequency expansion

For small pumping amplitudes and frequencies, it is possible to derive an approximate expression for the dc current that is accurate up to $O(V^2)$ and up to $O(\Omega_0)$. Such a procedure would correspond to a generalized adiabatic approximation within the present formalism and will allow us to get analytical expressions to gain insight into the behavior of the dc current.

As a first step, we truncate the harmonics of the induced potentials up to $\varepsilon_0^{\rm eff}(0)$ and $\varepsilon_0^{\rm eff}(1)=[\varepsilon_0^{\rm eff}(-1)]^*=V_{\rm eff}$, and the harmonics of the self-energy up to $\Sigma(0,\omega)$ [higher harmonics involve terms $O(V^2)$ and $O(U^2V)$]. The Dyson's equation for the retarded Green's function reads

$$G^R_{l,l'}(t,\omega) \sim G^0_{l,l'}(\omega) + \sum_{j=-1}^{1} G^R_{l,j}(t,\omega+\Omega_0)\varepsilon_j^{\rm eff}(1)e^{-i\Omega_0 t}G^0_{j,l'}(\omega) + \sum_{j=-1}^{1} G^R_{l,j}(t,\omega-\Omega_0)\varepsilon_j^{\rm eff}(-1)e^{i\Omega_0 t}G^0_{j,l'}(\omega), \quad (12)$$

where the pumping potentials contain the external time-dependent fields as well as the time-dependent potential induced by the interactions:

$$\varepsilon_j^{\rm eff}(1) = V(\delta_{j,-1}e^{-i\varphi} + \delta_{j,1}) + V_{\rm eff}\delta_{j,0}, \quad (13)$$

with $[\varepsilon_j^{\rm eff}(1)]^*=\varepsilon_j^{\rm eff}(-1)$. The Green's functions $G^0_{l,l'}(\omega)$ correspond to the stationary part of the Hamiltonian. The solution of (13) up to the first order in $\varepsilon_j^{\rm eff}(k)$ gives

$$G^R_{l,l'}(t,\omega) = \sum_{k=-1}^{1} \mathcal{G}_{l,l'}(0,\omega)e^{-ik\omega_0 t}, \quad (14)$$

with

$$\mathcal{G}_{l,l'}(0,\omega) = G^0_{l,l'}(\omega).$$

$$\mathcal{G}_{l,l'}(\pm 1,\omega) = \sum_{j=-1}^{1} G^0_{l,j}(\omega\pm\Omega_0)\varepsilon_j^{\rm eff}(\pm 1)G^0_{j,l'}(\omega). \quad (15)$$

Equation (9) leads, within this approximation, to the following self-consistency condition to evaluate $V_{\rm eff}$:

$$V_{\rm eff} = U\sum_{\alpha=L,R,j=-1}^{1}\int_{-\infty}^{\infty}\frac{d\omega}{2\pi}\Gamma_0(\omega)f(\omega)\varepsilon_j^{\rm eff}(1) \times[G^0_{0,j}(\omega+\Omega_0)G^0_{j,l_\alpha}(\omega)G^0_{0,l_\alpha}(\omega)^* + G^0_{0,l_\alpha}(\omega)G^0_{0,j}(\omega)^*G^0_{j,l_\alpha}(\omega-\Omega_0)^*]. \quad (16)$$

A rough estimate of the pumping potential *without self-consistency* is

$$\varepsilon_0^{(0)}(1) \sim UV\lambda_0(1+e^{-i\varphi}), \quad (17)$$

where

$$\lambda_0 = \int_{-\infty}^{\infty}\frac{d\omega}{2\pi}\sum_{\alpha=L,R}\int_{-\infty}^{\infty}\frac{d\omega}{2\pi}\Gamma_0(\omega)f(\omega) \times[G^0_{0,1}(\omega+\Omega_0)G^0_{1,j_\alpha}(\omega)G^0_{0,j_\alpha}(\omega)^* + G^0_{0,j_\alpha}(\omega)G^0_{0,1}(\omega)^*G^0_{1,j_\alpha}(\omega-\Omega_0)^*]. \quad (18)$$

Thus, within this rough approximation, $V_{\rm eff}\sim\varepsilon_0^{(0)}(1)=UV\lambda_0[1+\cos(\varphi)-i\sin(\varphi)]$. Within the self-consistent procedure, however, $V_{\rm eff}=V'_{\rm eff}+iV''_{\rm eff}$, with both real and imaginary parts of the form $V'^{(\prime\prime)}_{\rm eff}\sim A_0'^{(\prime\prime)}\sin(\varphi)+A_1'^{(\prime\prime)}[1+\cos(\varphi)]$. On the other hand, on expanding the above expressions up to the first order in Ω_0 we find $V_{\rm eff}\sim V^0_{\rm eff}+V^1_{\rm eff}\Omega_0$.

Expanding (3) in powers of Ω_0 gives for the first-order contribution

$$J^{\rm dc} \sim J^{\rm el} \sim \Omega_0\Gamma^2(\mu)\sum_{k=-1}^{1} k[|\mathcal{G}_{1,1}(k,\mu)|^2 - |\mathcal{G}_{-1,-1}(k,\mu)|^2 + |\mathcal{G}_{1,-1}(k,\mu)|^2 - |\mathcal{G}_{-1,1}(k,\mu)|^2]. \quad (19)$$

Substituting the zeroth-order term in Ω_0 of (15) into (20), we find

$$J^{\rm el} \sim \Omega_0\Gamma^2(\mu)\sum_{j\neq l}[\varepsilon_j^{\rm eff}(1)\varepsilon_l^{\rm eff}(1)^* - \varepsilon_j^{\rm eff}(-1)\varepsilon_l^{\rm eff}(-1)^*](\lambda_{lj} - \lambda_{jl}), \quad (20)$$

where

$$\lambda_{jl} = \sum_{l_\alpha=\pm 1} l_\alpha G^0_{l_\alpha,j}(\mu)G^0_{l_\alpha,l}(\mu)^*\gamma_{lj}(l_\alpha),$$

$$\gamma_{lj}(-1) = \sum_{l_\alpha=\pm 1} G^0_{j,l_\alpha}(\mu) G^0_{l,l_\alpha}(\mu)^*,$$

$$\gamma_{lj}(1) = \sum_{l_\alpha=\pm 1} G^0_{j,l_\alpha}(\mu) G^0_{l,-l_\alpha}(\mu)^*. \quad (21)$$

In the case of the rough estimate for the induced pumping potential $\varepsilon_0^{(0)}(1)$ defined above, a relation between the current and the phase lag of the form $J^{\rm el} \propto \sin(\varphi)$, as in the noninteracting case, is obtained. However, when the pumping potential is evaluated self-consistently, the current behaves as follows:

$$J^{\rm dc} \sim J^{\rm el} \sim \Omega_0 \frac{(\Gamma^{\rm el})^2}{(\Gamma_0)^4} V(V \sin(\varphi)\lambda_1^{\rm el} + \{V_0' \sin(\varphi)[\cos(\varphi)+1] + V_0'' \sin^2(\varphi)\}\lambda_2^{\rm el}), \quad (22)$$

where we have defined $\Gamma^{\rm el}=\Gamma(\mu)$; here $\Gamma_0=4|w|^2/\Gamma(\mu)$, which is approximately the effective tunneling rate from the interacting site to the leads. The dimensionless functions $\lambda_i^{\rm el}$ as well as V_0' and V_0'' depend on $V_{\rm eff}$ and on the parameters λ_{lj} of Eq. (21). It is important to note that Eq. (22) reduces to the noninteracting result $J^{\rm dc} \sim V^2 \sin(\varphi)$ originally proposed in Ref. 8 for $V_0'=V_0''=0$. Such a dependence on φ has been observed experimentally in Ref. 1 and is a manifestation of quantum interference between processes of coherent emission and absorption of quanta at the two pumping centers. In the interacting system the terms proportional to $\lambda_2^{\rm el}$ of Eq. (22) are a consequence of additional interference with scattering events at the pumping center induced by the interactions.

The inelastic contribution exhibits the same structure, except for a different prefactor $\Gamma^{\rm in}=-2\,{\rm Im}[\Sigma_0^{\rm eq}(\mu)]$, where $\Sigma_0^{\rm eq}(\omega) \sim \Sigma_0^R(0,\omega)$ is the SOSE of the system with $V=0$, instead of $\Gamma^{\rm el}$. For low T, $\Gamma^{\rm in} \sim (\omega-\mu)^2$; thus, for low Ω_0, $J^{\rm in} \sim 0$ and the elastic processes account for the full dc transport.

IV. RESULTS

A. Weakly interacting regime

We begin with the analysis of the effect of the interactions in the behavior of $J^{\rm dc}$ as a function of Ω_0 at $T=0$ for a given chemical potential μ and phase lag φ. In Fig. 2 we present the behavior of the different contributions to $J^{\rm dc}$ obtained from the numerical solution of the full Dyson's equation, retaining the self-energy components $\Sigma_0^{>,<}(k,\omega)$ up to $|k|=2$, with a self-consistent evaluation of $\varepsilon_0^{\rm eff}(0)$, and $\varepsilon_0^{\rm eff}(1) \equiv V_{\rm eff}$. Energies, frequencies, and currents are expressed in units of Γ_0. The inset shows the corresponding local density of states at the interacting site $\rho_0(\omega)=-2\,{\rm Im}[\mathcal{G}_{0,0}(0,\omega)]$ along with the density of states corresponding to the noninteracting system ($U=0$). The position of the resonant peak is shifted by $\varepsilon_{\rm eff}(0)$ with respect to the noninteracting one. For low U the effects of $\Sigma(k,\omega)$ are vanishingly small and the description effectively reduces to the TDHF approximation. The induced $V_{\rm eff}$ is also very small ($V_{\rm eff} \sim 1\times 10^{-3} \ll V$). For low U, the inelastic contribution to the current $[O(U^2)]$ is negligible. Therefore, within this regime, $J^{\rm dc}$ is qualitatively similar to the noninteracting result, shown as a dotted line. As the hybridization between the dot and the side reservoirs is sizable, the resonant peak is wide and the adiabatic (proportional to Ω_0) behavior is observed within a wide range of Ω_0.

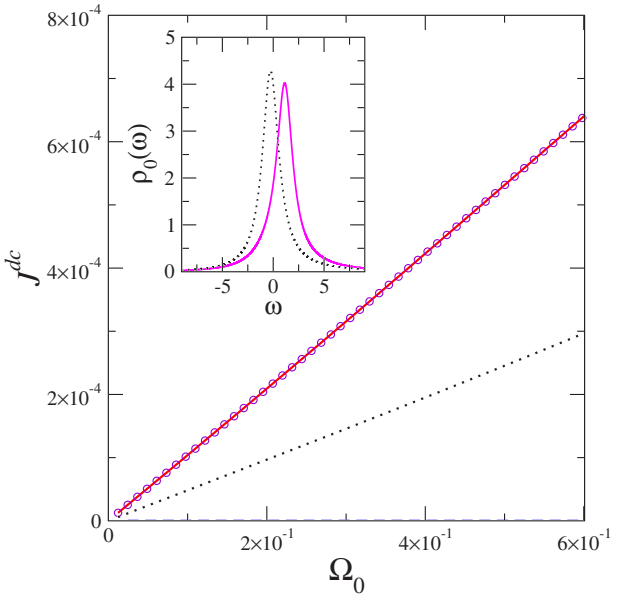

FIG. 2. (Color online) $J^{\rm el}$ (solid line), $J^{\rm in}$ (dashed line), and $J^{\rm dc}$ (circles) for $\varphi=\pi/2$, as functions of the driving frequency Ω_0 for $U=1$. The inelastic component is $J^{\rm in} \sim 0$. The dc current for the noninteracting system ($U=0$) is also shown as a dotted line for comparison. The corresponding local densities of states at the interacting site $\rho_0(\omega)$ are indicated in the inset (solid lines), along with the noninteracting one (dotted line). Other parameters are $E=2$, $w=2$, $w_c=8$, $V=0.4$, and $\mu=2$. (Energies, frequencies, and currents are expressed in units of Γ_0.)

B. Kondo regime

Let us now analyze the more subtle Kondo regime, which occurs at higher U. In Fig. 3 we show a series of plots similar to those of Fig. 2 but corresponding to a value of U for which the Kondo effect takes place. For these parameters, the density of states at the interacting site $\rho_0(\omega)$ exhibits the characteristic Kondo resonance at the Fermi energy $\omega=\mu$ with two high-energy side features distant by an energy $\pm U$, as shown in the inset of the figure. At this point it is important to recall that, due to the presence of barriers in the structure, our model is not particle-hole symmetric. For this reason, the profile of $\rho_0(\omega)$ is not symmetric with respect to $\omega=0$, in contrast to the one we are used to seeing in the usual Kondo regime. As a function of Ω_0, the behavior of $J^{\rm dc}$ significantly departs from the noninteracting one in this regime and there are several issues needing comment in connection with Fig. 3. First, it is clear that self-energy effects now play an important role. This is evident in the drastic changes displayed by the density of states as well as in the fact that the current departs from the behavior predicted by the TDHF approximation, which is shown as a light dot-dashed line in the figure.

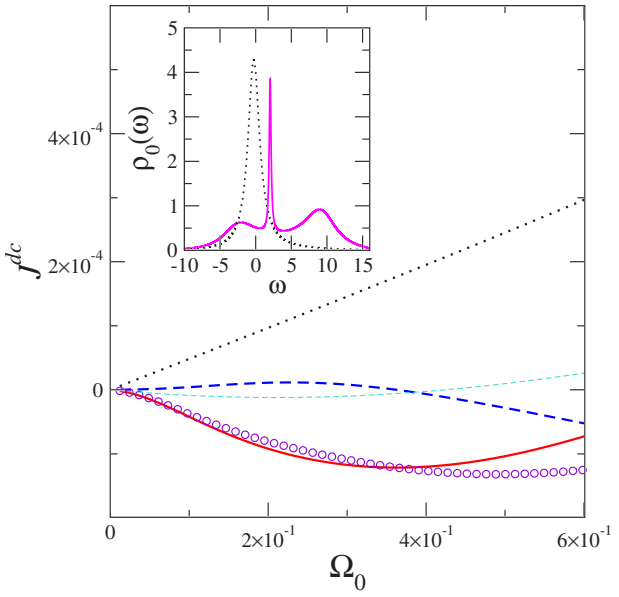

FIG. 3. (Color online) J^{el} (solid line), J^{in} (dashed line), and J^{dc} (circles) for $\varphi=\pi/2$, as functions of the driving frequency Ω_0 for $U=10$. The details are the same as in Fig. 2. The local density of states $\rho_0(\omega)$ at the interacting site for $\Omega_0=0.1$ is shown as a solid line in the inset, where the corresponding density of states for the noninteracting system is also shown as a dashed line for comparison.

The second feature to remark is that, although inelastic processes are negligible for low Ω_0, as discussed in Sec. III C, they become sizable as Ω_0 increases, even at $T=0$ (see dashed line of the main frame of Fig. 3).

The third remarkable issue is the loss of the adiabatic behavior, namely, the departure from the linear dependence on Ω_0. We identify two ingredients that contribute to this effect. (i) The first one is the induced pumping potential at the interacting site, which becomes sizable $V_{\text{eff}}>1\times10^{-2}$ and changes significantly with Ω_0. This feature manifests itself even at the TDHF level [see Eq. (16)], in which case the range of pumping frequencies where $J^{\text{dc(TDHF)}}\propto\Omega_0$ becomes very narrow ($\Omega_0<2\times10^{-2}$). (ii) The other ingredient is the development of the Kondo resonance. Recalling that the underlying assumption for low-frequency expansions like the one leading to Eq. (22) is that the typical width of the energy levels of the structure is $\tau^{-1}\gg\Omega_0$, it can be understood that the reduction of the width of the resonant level due to the Kondo effect originates a concomitant reduction of the range of Ω_0 where the adiabatic behavior is observed. For the parameters of Fig. 3, which correspond to $T_K\sim0.5$, such linear behavior is not captured even close to the lowest pumping frequency considered ($\Omega_0=1\times10^{-2}$).

The final issue worthy of mention is the inversion in the sign of the current with respect to the noninteracting case. In general, even in the simpler case of a system without many-body interactions, the issue of the sign of the current is one of the most delicate features to predict in a problem of quantum pumping. In the case of structures with low hybridization with the contacts, presenting a landscape of well-separated resonances, the issue of the sign of the current has been analyzed in detail in Refs. 10, 17, and 20. In those works, the origin for the sign inversion of the current has been identified as the interference between two resonant electronic levels mixed by a high pumping frequency. In order to gain insight into the different processes involved in the present problem, let us first analyze the behavior of the sign of the current in the noninteracting limit of our setup of Fig. 1. In that case the dc current (2) can also be written as follows:[17]

$$J^{\text{dc}}_{\text{nonint}}=\int_{-\infty}^{+\infty}d\omega\, f(\omega)T(\omega), \tag{23}$$

where the "transmission" function $T(\omega)$ depends on the Green's functions of the system with $U=0$. Plots of the function $T(\omega)$ and its integral between $-\infty$ and μ, which is equivalent to $J^{\text{dc}}_{\text{nonint}}$ at zero temperature for two different hybridizations w_c, are shown in Fig. 4. In the upper panels, corresponding to a small w_c, three features can be distinguished, associated with the three eigenvalues of the tight-binding structure with three sites $l=-1,0,1$. In contrast, for

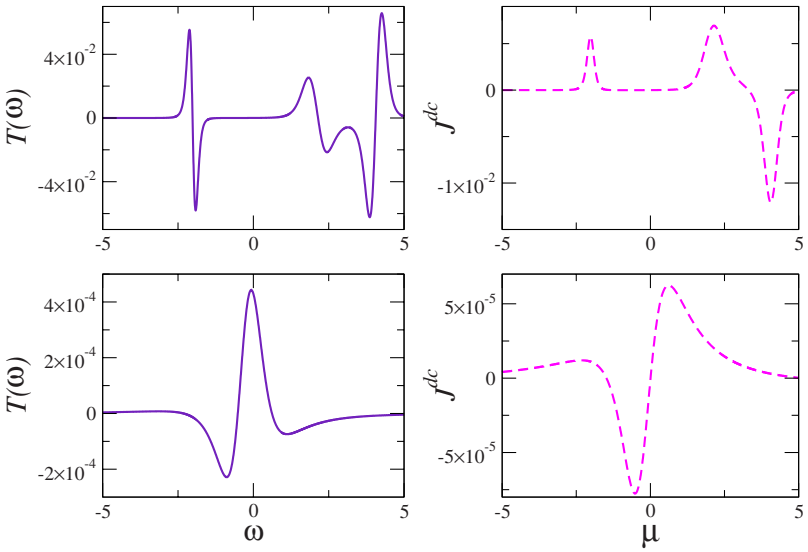

FIG. 4. (Color online) Transmission function $T(\omega)$ for a noninteracting structure with $\Omega_0=0.1$ and $w_c=0.64$ (upper left panel) and $w_c=8$ (lower left panel). Other details are the same as in Fig. 2.

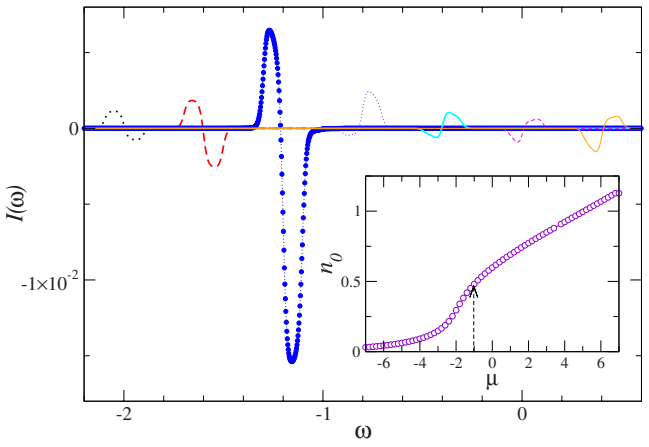

FIG. 5. (Color online) Integrand $I(\omega)$ for $\Omega_0=0.1$ and $U=10$. Different plots correspond to different equidistant values of the chemical potential $-2\leq\mu\leq0.4$. In the inset, the mean occupation per spin of the dot is shown as a function of the chemical potential. Other parameters are as in Fig. 2.

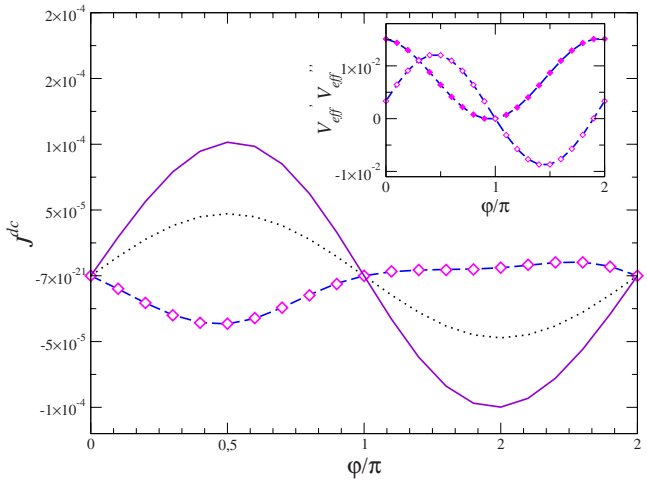

FIG. 6. (Color online) J^{dc} for $\Omega_0=0.1$ as a function of the phase lag φ for $U=1$ (thick solid line), and 10 (thick dashed line). The current corresponding to the noninteracting dot (with $U=0$) is shown as a dotted line, for comparison. The symbols are fits with the function $A_0\sin(\varphi)+A_1\sin^2(\varphi)+A_2\sin(\varphi)[1+\cos(\varphi)]$, suggested by Eq. (22). Inset: Effective potential $V_{\text{eff}}=V'_{\text{eff}}+iV''_{\text{eff}}$ along with fits as symbols with the function $A_0\sin(\varphi)+A_1[1+\cos(\varphi)]$. Other details are as in Fig. 2.

the higher w_c chosen to capture the Kondo regime used in Figs. 2 and 3, the three levels of the uncoupled structure are mixed and only one feature can be distinguished. As a consequence of the ensuing combination of quantum states, the transmission function as well as the current change sign within a wide range of μ with respect to the weakly coupled structure.

In the case of the interacting system, we analyze the behavior of the function $I(\omega)=\Sigma_k[I^{\text{el}}(k,\omega)+I^{\text{in}}(k,\omega)]$, which, when integrated over ω, gives the total dc current. The behavior of this function within the Kondo regime is shown in Fig. 5. Unlike the function $T(\omega)$ defined for the noninteracting system, the function $I(\omega)$ changes as the chemical potential changes. For this reason, several plots corresponding to different values of the chemical potential, for which we have verified that the Kondo resonance is developed, are shown in the figure. For each μ there is a feature in $I(\omega)$ around $\omega\sim\mu$ that precisely indicates the electronic transmission through the Kondo resonance. Notice that these features are very narrow and resemble the lowest-energy plot of the upper left panel of Fig. 4, which corresponds to a resonance for a dot with low hybridization with the reservoirs. Interestingly, for $\mu\sim-1$, $I(\omega)$ displays a phase shift of π, leading to a concomitant change of sign in the dc current. This particular value of the chemical potential corresponds to a charge population per spin of the dot $n_0\equiv n_{0,\sigma}^{\text{SOSE}}(0)\sim1/2$.

We show in Fig. 6 the behavior of the dc current as a function of the phase lag. The limiting case of $U=0$ is plotted as a dotted line in Fig. 6. For low Coulomb interaction (see the solid thick line), the induced effective pumping potential is small and the behavior of the dc current is qualitatively the same as that corresponding to the noninteracting case. For increasing U, the induced pumping amplitude V_{eff} becomes sizable. Within the self-consistent procedure, this is a complex function of φ with real and imaginary parts V'_{eff} and V''_{eff} displaying the functional structure of φ suggested by the perturbative solution leading to Eq. (22). The ensuing curve J^{dc} vs φ also shows the pattern predicted by Eq. (22).

Notice that the dc current, as well as V_{eff}, can be fitted with an excellent degree of accuracy by functions of φ with the structure suggested by this equation (see symbols in Fig. 6). A striking feature observed in this figure as well as in the analytical expression (22) is the breaking of the symmetry $\varphi\rightarrow-\varphi$ in the behavior of the dc current. On general physical grounds, the symmetry of the problem in the case of identical pumping amplitudes at the two barriers indicates that $J^{\text{dc}}(\varphi)\rightarrow-J^{\text{dc}}(-\varphi)$. However, the many-body treatment adopted in the present work breaks such symmetry for high enough induced V_{eff}, even at the level of the simple self-consistent TDHF approximation, i.e., even disregarding self-energy effects. The self-consistent evaluation of higher harmonics (we recall that we truncate at $|k|=2$) and additional self-energy and vertex corrections that we have not taken into account are expected to restore such symmetry. In any case, our results should be interpreted as a piece of evidence for the departure from the $J^{\text{dc}}\propto\sin(\varphi)$ behavior induced by the interactions.

So far, we have focused on the case of temperature $T=0$, where inelastic effects play an insignificant role at low Ω_0. To complete our analysis, we analyze in what follows inelastic effects, which become relevant at all frequencies at finite T. The evolution of the dc current as a function of Ω_0 as the temperature grows within a range $0<T<T_K$ is analyzed in Fig. 7. At first glance, it becomes apparent that the dominant contribution at low Ω_0 is J^{el} at the lowest T, while it becomes J^{in} for the highest ones. The elastic contribution vanishes as the Kondo resonance disappears, while the inelastic one increases due to the corresponding growth of Γ^{in}. The latter increment translates into the inverse time τ^{-1}, thus increasing the range of Ω_0 where the behavior $J^{\text{dc}}\propto\Omega_0$ holds. In fact, notice that the range of low Ω_0 where the plots of Fig. 4 look horizontal increases with increasing T.

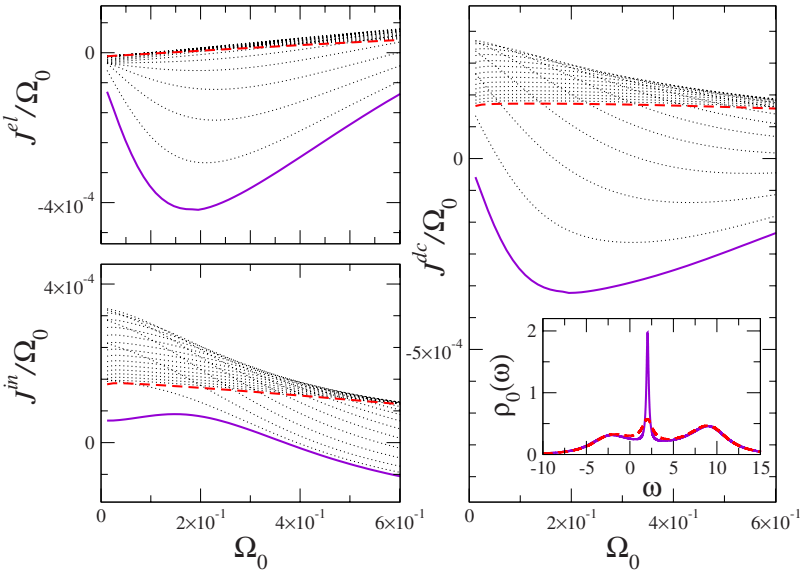

FIG. 7. (Color online) J^{el}/Ω_0 (top left), J^{in}/Ω_0 (bottom left), and J^{dc}/Ω_0 (right) as functions of the pumping frequency Ω_0 for 20 values of equally spaced temperatures in the range $0.04 \leq T/T_K \leq 0.8$ and Coulomb interaction $U = 10$. The lowest and highest temperatures are indicated as thick solid and dashed lines, respectively. The local density of states of the dot, $\rho_0(\omega)$, is depicted in the inset for the lowest and highest temperatures. Other details are as in Fig. 2.

V. SUMMARY AND CONCLUSIONS

To conclude, we have analyzed a simple model for an interacting quantum pump by means of nonequilibrium Green's function techniques and within a second-order self-energy approximation. We have shown that the effective time-dependent scattering center induced by the interactions generates interference effects, which should be detectable in a J^{dc} vs φ experimental curve, following the pattern predicted by Eq. (22). We have shown that the Kondo effect manifests itself in the J^{dc} vs Ω_0 behavior, which could also be detectable in future experiments. Below the Kondo temperature T_K, the Kondo resonance enables the elastic transport of electrons; however, the frequency range within which J^{dc} behaves linearly in Ω_0 is extremely narrow. We have identified two different ingredients as the origin of this feature: (i) on the one hand, the width of the Kondo resonance sets a narrow bound on the pumping frequencies in which the adiabatic behavior occurs and (ii) on the other hand, the induced pumping potential at the interacting site itself displays a sizable change in Ω_0, which propagates in the behavior of the current. As the temperature grows, inelastic scattering becomes dominant and the range where $J^{dc} \propto \Omega_0$ becomes wider.

ACKNOWLEDGMENTS

We thank C. Urbina and J. Splettstoesser for constructive comments. We acknowledge support from CONICET, Argentina, Grant No. FIS2006-08533-C03-02, the "RyC" program from MCEyC, Groups of Excellence of Spain Grant No. DGA, and the hospitality of Boston University (L.A.), as well as MCEyC, Spain, Grant No. FIS2005-06255 (A.L.Y. and A.M.R.).

[1] M. Switkes, C. M. Marcus, K. Campman, and A. C. Gossard, Science **283**, 1905 (1999).
[2] L. J. Geerligs, V. F. Anderegg, P. A. M. Holweg, J. E. Mooij, H. Pothier, D. Esteve, C. Urbina, and M. H. Devoret, Phys. Rev. Lett. **64**, 2691 (1990); L. DiCarlo, C. M. Marcus, and J. S. Harris, *ibid.* **91**, 246804 (2003).
[3] M. D. Blumenthal, B. Kaestner, L. Li, S. Giblin, T. J. B. M. Hanssen, M. Pepper, D. Anderson, G. Jones, and D. A. Ritchie, Nat. Phys. **3**, 343 (2007).
[4] D. Goldhaber-Gordon *et al.*, Nature (London) **391**, 156 (1998).
[5] B. Babic, T. Kontos, and C. Schonenberger, Phys. Rev. B **70**, 235419 (2004); P. Jarillo-Herrero *et al.*, Nature (London) **434**, 484 (2005).
[6] P. M. Billangeon, F. Pierre, H. Bouchiat, and R. Deblock, Phys. Rev. Lett. **98**, 126802 (2007); S. Russo, J. Tobiska, T. M. Klapwijk, and A. F. Morpurgo, *ibid.* **99**, 086601 (2007).
[7] M. Büttiker, H. Thomas, and A. Prêtre, Z. Phys. B: Condens. Matter **94**, 133 (1994).
[8] P. W. Brouwer, Phys. Rev. B **58**, R10135 (1998).
[9] P. W. Brouwer, Phys. Rev. B **63**, 121303(R) (2001); M. L. Polianski and P. W. Brouwer, *ibid.* **64**, 075304 (2001).
[10] M. Moskalets and M. Büttiker, Phys. Rev. B **66**, 205320 (2002); **69**, 205316 (2004).
[11] I. L. Aleiner and A. V. Andreev, Phys. Rev. Lett. **81**, 1286 (1998); F. Zhou, B. Spivak, and B. Altshuler, *ibid.* **82**, 608 (1999); J. E. Avron, A. Elgart, G. M. Graf, and L. Sadun, Phys. Rev. B **62**, R10618 (2000); Phys. Rev. Lett. **87**, 236601 (2001); J. Math. Phys. **43**, 3415 (2002); O. Entin-Wohlman, A. Aharony, and Y. Levinson, Phys. Rev. B **65**, 195411 (2002); V. Kashcheyevs, A. Aharony, and O. Entin-Wohlman, *ibid.* **69**, 195301 (2004).
[12] B. Wang and J. Wang, Phys. Rev. B **65**, 233315 (2002); M. N. Kiselev, K. Kikoin, R. I. Shekhter, and V. M. Vinokur, *ibid.* **74**, 233403 (2006); E. Sela and Y. Oreg, Phys. Rev. Lett. **96**, 166802 (2006).
[13] T. Aono, Phys. Rev. Lett. **93**, 116601 (2004); J. Splettstoesser,

M. Governale, J. König, and R. Fazio, *ibid.* **95**, 246803 (2005).
[14] A. Schiller and A. Silva, Phys. Rev. B **77**, 045330 (2008); D. Fioretto and A. Silva, arXiv:0707.3338 (unpublished).
[15] K. Das, arXiv:0710.2953 (unpublished).
[16] A. L. Yeyati, A. Martin-Rodero, and F. Flores, Phys. Rev. Lett. **71**, 2991 (1993).
[17] L. Arrachea, Phys. Rev. B **72**, 125349 (2005); **75**, 035319 (2007).
[18] A. Oguri, Phys. Rev. B **52**, 16727 (1995); R. López, R. Aguado, G. Platero, and C. Tejedor, Phys. Rev. Lett. **81**, 4688 (1998); A. L. Yeyati, F. Flores, and A. Martín-Rodero, *ibid.* **83**, 600 (1999).
[19] L. Arrachea and M. Moskalets, Phys. Rev. B **74**, 245322 (2006).
[20] L. Arrachea, C. Naón, and M. Salvay, Phys. Rev. B **76**, 165401 (2007).